

Energy scales of $\text{Lu}_{1-x}\text{Yb}_x\text{Rh}_2\text{Si}_2$ by means of thermopower investigations

U. Köhler,* N. Oeschler, and F. Steglich

Max Planck Institute for Chemical Physics of Solids, D-01187 Dresden, Germany

S. Maquilon and Z. Fisk

Department of Physics and Astronomy, University of California, Irvine, California 92697, USA

(Received 17 October 2007; revised manuscript received 1 February 2008; published 11 March 2008)

We present the thermopower $S(T)$ and the resistivity $\rho(T)$ of $\text{Lu}_{1-x}\text{Yb}_x\text{Rh}_2\text{Si}_2$ in the temperature range $3 < T < 300$ K. $S(T)$ is found to change from two minima for dilute systems ($x < 0.5$) to a single large minimum in pure YbRh_2Si_2 . A similar behavior has also been found for the magnetic contribution to the resistivity $\rho_{\text{mag}}(T)$. The appearance of the low- T extrema in $S(T)$ and $\rho_{\text{mag}}(T)$ is attributed to the lowering of the Kondo scale $k_B T_K$ with decreasing x . The evolution of the characteristic energy scales for both the Kondo effect and the crystal electric field splitting Δ_{CEF} are deduced. An extrapolation of T_K to $x=1$ allows us to estimate the Kondo temperature of YbRh_2Si_2 to 29 K. For pure YbRh_2Si_2 , T_K and Δ_{CEF}/k_B lie within one order of magnitude and thus the corresponding extrema merge into one single feature.

DOI: 10.1103/PhysRevB.77.104412

PACS number(s): 72.15.Jf, 72.15.Eb, 75.20.Hr, 71.70.Ch

I. INTRODUCTION

YbRh_2Si_2 is a stoichiometric heavy-fermion (HF) metal with an extremely low antiferromagnetic ordering temperature of 70 mK.¹ It crystallizes in the tetragonal ThCr_2Si_2 structure and has been investigated extensively due to its pronounced non-Fermi liquid (NFL) properties at low T . This behavior was attributed to a quantum critical point, which can be attained by application of a small magnetic field of 60 mT within the ab plane.² At intermediate temperatures (10–300 K), the properties of YbRh_2Si_2 are determined by a competition of crystal electric field (CEF) excitations and the Kondo interaction. A knowledge of the corresponding characteristic energy scales $k_B T_{\text{CEF}}$ and $k_B T_K$ is essential for an understanding of the low-temperature properties of the compound. The NFL behavior dominates the thermodynamic and transport properties up to 10 K. Notably, the electronic specific heat divided by T exhibits a logarithmic increase upon cooling with a spin fluctuation temperature $T_0=24$ K.¹ The corresponding entropy revealed a doublet ground state of the Yb^{3+} ions with a Kondo temperature T_K of approximately 17 K.³ The CEF level scheme of YbRh_2Si_2 was determined from inelastic neutron scattering: The $4f^{13}$ multiplet of the Yb^{3+} is split into four doublets at energies corresponding to 0–200–290–500 K, respectively.⁴

The strong interplay between Kondo effect and CEF splitting manifests itself in the transport properties of the system. The temperature dependencies of both resistivity⁵ $\rho(T)$ and thermopower⁶ $S(T)$ exhibit a single large extremum around 100 K, which was attributed to scattering on the full Yb^{3+} multiplet. No signature corresponding to Kondo scattering on the ground-state doublet at T_K has been found in $S(T)$ and $\rho(T)$. Such behavior was observed and theoretically predicted for compounds, where the energy scales $k_B T_{\text{CEF}}$ and $k_B T_K$ are of the same order of magnitude, i.e., for systems near the crossover from the HF to the intermediate-valent (IV) regime.^{7–9}

Upon applying pressure, the Kondo temperature of Yb-based HF systems is typically shifted to lower T , while the

CEF levels are not affected significantly. For sufficiently small values of T_K , separate maxima in $\rho(T)$ due to Kondo effect on the ground state and on excited CEF levels are expected to occur. Such behavior was confirmed for YbRh_2Si_2 by means of resistivity investigations under pressure:⁵ Above 4 GPa, the single peak in $\rho(T)$ splits into three separate maxima. The two maxima at lower T were attributed to Kondo scattering on the ground-state doublet with the onset of coherence and to Kondo scattering on thermally populated CEF levels. The origin of a third maximum remains unclear.

According to theoretical models, the lowering of T_K is also expected to induce systematic changes in $S(T)$ (Ref. 8 and references therein): For systems with a thermopower as described for YbRh_2Si_2 , the anticipated behavior upon application of a small pressure or weak lowering of T_K is the appearance of a low- T shoulder. With further decreasing T_K , two separate minima develop in $S(T)$, similar to the behavior of $\rho(T)$. The minimum at lower T , which reflects Kondo scattering on the ground-state doublet, is situated at $T_{\text{min}1} \approx T_K$.^{8,10,11} The high- T minimum is caused by Kondo scattering on thermally populated CEF levels. For an excited CEF level at Δ_{CEF} above the ground state, it typically appears at $T_{\text{min}2} \approx (0.3–0.6)\Delta_{\text{CEF}}/k_B$.^{8,12,13} Such evolution has been detected, e.g., for $\text{Yb}(\text{Ni}_x\text{Cu}_{1-x})_2\text{Si}_2$ upon substitution (chemical pressure).¹⁴ The IV system YbCu_2Si_2 exhibits a single minimum in $S(T)$. As the Kondo temperature is reduced by Ni substitution on the Cu site, a shoulder appears at low T already for the lowest Ni content studied ($x=0.125$). However, it remains unsolved, whether only a single minimum occurs, when the system is pushed to the HF regime for Ni concentrations $x < 0.125$, or whether the appearance of the low- T shoulder is directly related to the development of the HF state. YbRh_2Si_2 seems to be an appropriate system to address this problem, since it, being a HF metal, exhibits a single minimum in $S(T)$.

In order to change the effective coupling between the $4f$ and the conduction electrons, substitution on all crystallographic sites has been realized in YbRh_2Si_2 , generally with

the aim of lowering the antiferromagnetic ordering temperature. This, however, is connected with an increase in T_K as observed in $\text{La}_{1-x}\text{Yb}_x\text{Rh}_2\text{Si}_2$,¹⁵ I-type YbIr_2Si_2 ,¹⁶ and $\text{YbRh}_2(\text{Si}_{1-y}\text{Ge}_y)_2$.¹⁷ Recent investigations on $\text{Lu}_{1-x}\text{Yb}_x\text{Rh}_2\text{Si}_2$ indicate a weak lowering of T_K upon replacement of Yb by the nonmagnetic Lu.¹⁸ Additionally, the substitution on the Yb site leaves, in a first approximation, the chemical environment of the remaining Yb ions unchanged, thus reducing the influence of disorder on the magnetic moments. $\text{Lu}_{1-x}\text{Yb}_x\text{Rh}_2\text{Si}_2$ therefore appeared a promising candidate for the observation of distinct anomalies in the thermopower due to Kondo interaction on the ground state and on excited CEF levels at ambient pressure, with the objective to determine the characteristic energy scales $k_B T_K$ and $k_B T_{\text{CEF}}$ of pure YbRh_2Si_2 .

In this paper, we present thermopower and resistivity measurements of a number of $\text{Lu}_{1-x}\text{Yb}_x\text{Rh}_2\text{Si}_2$ single crystals with Yb concentration $0 \leq x \leq 1$. The energy scales of Kondo interaction and CEF excitations as a function of the Yb concentration are deduced based on the thermopower and supported by the resistivity data. Finally, the evolution of $S(T)$ and $\rho(T)$ is discussed in comparison to other Ce- and Yb-based materials.

II. EXPERIMENTAL DETAILS

Single crystals of $\text{Lu}_{1-x}\text{Yb}_x\text{Rh}_2\text{Si}_2$ ($0 \leq x < 1$) were grown from In flux, as described elsewhere.¹⁸ The average (nominal) Yb content x_{nom} of each batch was determined from susceptibility measurements and confirmed by microprobe analysis on selected crystals. However, our resistivity measurements suggest a moderate variation of the Yb concentration throughout a batch. The scaling analysis described below indicates deviations from x_{nom} of up to approximately 5%. Specifically, the samples with $x_{\text{nom}}=0.15$ and $x_{\text{nom}}=0.49$ studied in $S(T)$ and $\rho(T)$ have an effective Yb concentration of $x=0.10$ and $x=0.44$, respectively. For all other samples, the nominal concentration has been confirmed, i.e., $x=x_{\text{nom}}$. In the following, the effective values x are used.

The lattice constants of the stoichiometric systems LuRh_2Si_2 and YbRh_2Si_2 were determined from x-ray diffraction measurements on powdered material. The ThCr_2Si_2 crystal structure has been confirmed within the doping series. No additional peaks have been resolved in the pattern. The fraction of foreign phases can thus be excluded to be higher than 2%. The microprobe analysis has indicated no free elemental nor binary phases in the studied samples. Due to the extremely small change of the unit-cell volume V_{uc} of $(0.41 \pm 0.12)\%$ with respect to YbRh_2Si_2 a linear dependence of $V_{\text{uc}}(x)$ is assumed for the crystals with partial substitution. The tiny variation in the lattice constant is not expected to significantly influence the relative position of the CEF levels.

Investigations of the thermopower S and the electrical resistivity ρ were performed within the ab plane of the crystals with a typical size of $4 \times 1 \times 0.05 \text{ mm}^3$. Both quantities were measured in the temperature range from 3 to 300 K in a commercial device (Physical Property Measurement System from Quantum Design) using the same contacts. Measure-

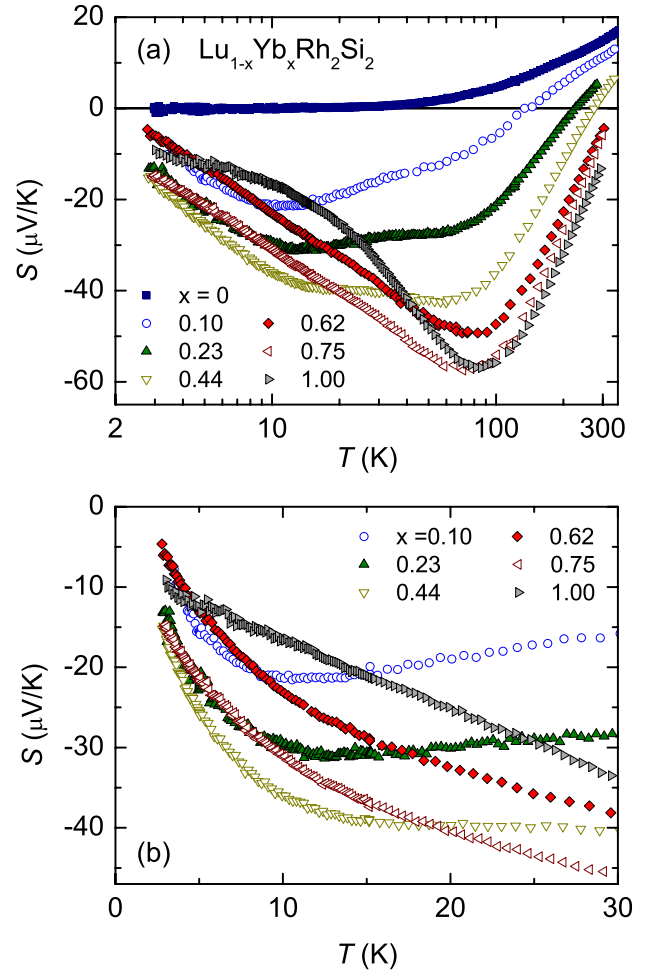


FIG. 1. (Color online) (a) Temperature dependence of the thermopower of $\text{Lu}_{1-x}\text{Yb}_x\text{Rh}_2\text{Si}_2$ ($0 \leq x \leq 1$). (b) Low-temperature behavior of $S(T)$ of the crystals with $x > 0$.

ments of ρ were extended down to 0.4 K using a ^3He insert. The resistivity was determined with a four-point ac technique. For the thermopower, a relaxation-time method with a low-frequency square-wave heat pulse utilizing two thermometers was used. The determination of S implies an average over the contact area of both the voltage and the temperature gradient. In our setup, due to the small crystal size, the contact size was not negligible compared to the sample dimensions. However, data sets obtained from repeated measurements on the same specimen but with different contacts can be scaled on top of each other. In particular, the position of the minimum in $S(T)$ remained unaffected. The absolute values of S could be reproduced within $\pm 8\%$. The thermopower data for the pure Yb compound are taken from Ref. 6.

III. RESULTS

The thermopower $S(T)$ of $\text{Lu}_{1-x}\text{Yb}_x\text{Rh}_2\text{Si}_2$ ($0 \leq x \leq 1$) is plotted semilogarithmically in Fig. 1(a) ($x=0.08$ not shown for the sake of clarity). Figure 1(b) displays the low- T behavior of the same curves on a linear temperature scale. The

thermopower of the reference compound LuRh_2Si_2 is smaller than $1 \mu\text{V}/\text{K}$ in this T range and therefore omitted.

LuRh_2Si_2 exhibits a small positive thermopower, which is typical for normal metals with hole-like charge carriers. The thermopower comprises mostly a diffusion part of light non-magnetic charge carriers. A strong phonon drag contribution leading to an enhancement around 20 K has not been resolved. By contrast, the thermopower of YbRh_2Si_2 is negative in the whole temperature range $3 \leq T \leq 300$ K with large absolute values. It shows a single broad minimum around 80 K, as typically found in valence-fluctuating Yb compounds such as YbCu_2Si_2 .¹⁴ However, for the HF system YbRh_2Si_2 , the observed behavior was attributed to a combination of Kondo interaction and CEF effects.⁶ With decreasing Yb concentration, the temperature dependence of the thermopower changes qualitatively. The samples with $x=0.75$ and $x=0.62$ exhibit a minimum at 80 K and a shoulder at low temperatures, which may be seen on a linear scale [Fig. 1(b)]. For Yb concentrations of $x \leq 0.44$, the thermopower minimum around 80 K clearly splits into two separate features. While the position of the high-temperature shoulder remains almost concentration independent, the low-temperature shoulder shifts to lower T upon further decreasing x . Simultaneously, the absolute values of the minimum structure at elevated temperatures are significantly reduced. For samples with $x \leq 0.44$, a sign change in $S(T)$ appears below room temperature, which is shifted to lower T with decreasing Yb concentration. This indicates a stronger relative influence of the nonmagnetic contribution to the thermopower in these samples.

The electrical resistivity of $\text{Lu}_{1-x}\text{Yb}_x\text{Rh}_2\text{Si}_2$ was measured on the same samples as the thermopower. In addition, a specimen with $x=0.02$ has been investigated, which was too small to measure $S(T)$. The results of $\rho(T)$ are in agreement with Ref. 18. The resistivity of LuRh_2Si_2 takes a value of about $30 \mu\Omega \text{ cm}$ at 300 K and decreases linearly from room temperature to 10 K, below which it reaches a constant value of $1.25 \mu\Omega \text{ cm}$. The magnetic contribution ρ_{mag} was calculated by subtracting the data of the reference compound LuRh_2Si_2 and a sample-dependent disorder term ρ_{dis}^0 . The results normalized to the Yb concentration are shown in Fig. 2. For most samples scaling of the data at elevated temperatures was achieved by using the value of the nominal concentration. As already mentioned above, adjustment of the effective concentration was necessary for $x_{\text{nom}}=0.15$ to $x=0.1$ and for $x_{\text{nom}}=0.49$ to $x=0.44$ to ensure scaling of the high- T data above 100 K.

The magnetic resistivity $\rho_{\text{mag}}(T)$ of the series reflects the evolution from a diluted to a dense Kondo system, as, e.g., demonstrated in $\text{Ce}_x\text{La}_{1-x}\text{Cu}_6$.¹⁹ At temperatures $T > 100$ K, ρ_{mag} of all samples increases logarithmically with decreasing T . Subsequently, samples with low Yb concentrations $x \leq 0.23$ exhibit a plateau around 60–100 K, followed by a further increase in ρ_{mag} to lower T . At $T < 4$ K, the magnetic resistivities of these specimens saturate. On the other hand, the magnetic resistivities of the concentrated Yb samples with $x \geq 0.62$ pass through maxima around 70–100 K and then drop toward lower temperatures. The plateau or maximum at elevated T is attributed to the presence of a CEF splitting in the system. The depopulation of excited levels

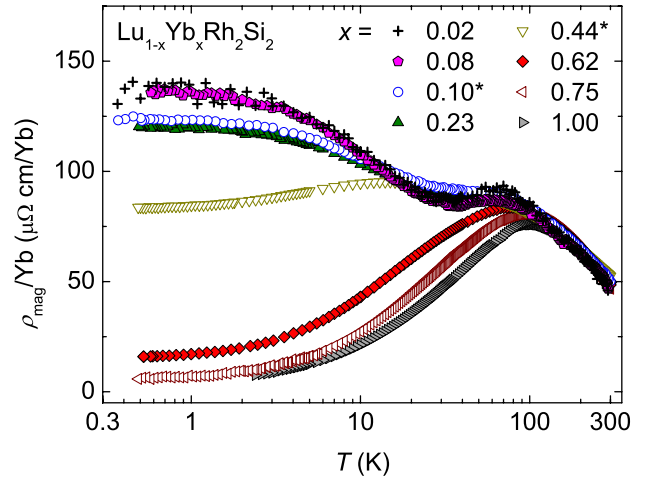


FIG. 2. (Color online) Temperature dependence of the magnetic contribution to the resistivity of $\text{Lu}_{1-x}\text{Yb}_x\text{Rh}_2\text{Si}_2$ ($0 < x \leq 1$). For samples denoted with an asterisk (*) the effective Yb concentration deviates from the nominal value, namely $x=0.44$ ($x_{\text{nom}}=0.49$) and $x=0.10$ ($x_{\text{nom}}=0.15$).

upon cooling and the associated lowering of the scattering rate leads to a reduction of ρ_{mag} in this temperature range. Toward lower T , the differences between the diluted and the dense Yb systems become evident. While Kondo scattering on the ground-state doublet gives rise to a second increase as $-\ln T$ and a saturation at lowest T for $x \leq 0.23$, the onset of coherence promotes a further decrease in the magnetic resistivity in samples with $x \geq 0.62$. The sample with Yb concentration $x=0.44$ is situated close to the crossover between the two regimes. It shows an only weak decrease in ρ_{mag} toward low T and a saturation at a relatively large residual value.

IV. DISCUSSION

For a quantitative analysis of the thermopower, the magnetic contribution S_{mag} is usually determined by use of the Gorter–Nordheim rule: $S_{\text{mag}}\rho_{\text{mag}} = S\rho - S_{\text{ref}}\rho_{\text{ref}}$. S_{ref} and ρ_{ref} are generally taken as the thermopower and (total) resistivity of the nonmagnetic reference compound. The resistivity ρ_{ref} may be approximated by a sum of a phononic contribution $\rho_{\text{ref}}^{\text{ph}}$ and a residual resistivity ρ_{ref}^0 due to impurities. It is assumed that $\rho_{\text{ref}}^{\text{ph}}$ does not change significantly upon chemical substitution. The disorder induced by doping, however, affects the residual resistivity, and ρ_{ref}^0 has to be replaced by the x dependent disorder contribution ρ_{dis}^0 of the alloys. Since $\rho_{\text{dis}}^0(x)$ cannot be determined accurately, an exact evaluation of S_{mag} is almost impossible. For the presented data, the overall behavior of S_{mag} , and especially the position of the shoulders, is not expected to strongly deviate from that of S . At low temperatures ($T < 50$ K), at which the thermopower and the resistivity of LuRh_2Si_2 are small, the difference between S and S_{mag} is negligible. Just below room temperature, the calculation of S_{mag} mainly implies a correction for the diffusion thermopower of light charge carriers. The features below 100 K remain basically unchanged. For the discussion of the data, we therefore analyze $S \approx S_{\text{mag}}$.

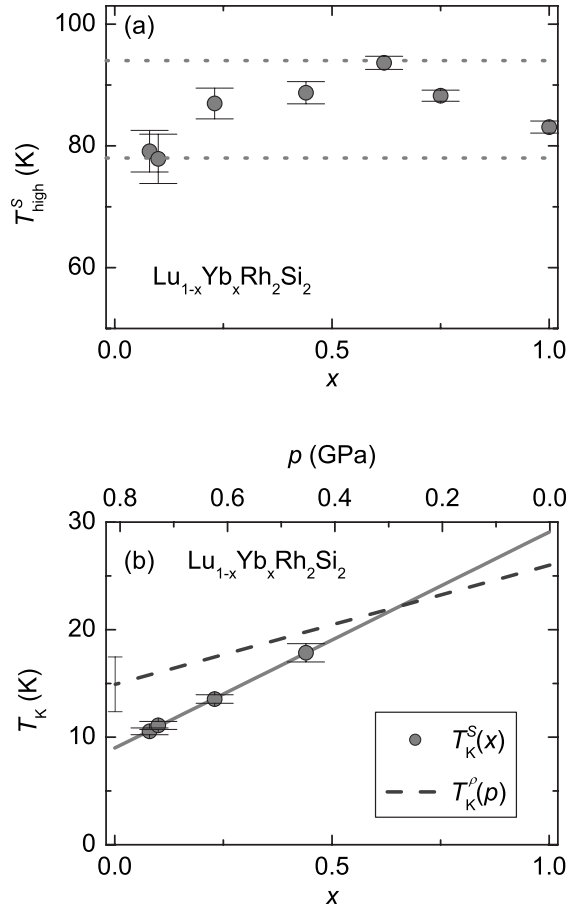


FIG. 3. Characteristic temperatures of [(a) and (b)] $\text{Lu}_{1-x}\text{Yb}_x\text{Rh}_2\text{Si}_2$ at ambient pressure and of (b) YbRh_2Si_2 under pressure. The x axes in (b) are scaled to the same unit-cell volume. The characteristic temperatures for $S(T)$ were obtained from a fit to the data as explained in the text. The error bars represent the uncertainty of the fitting procedure. The uncertainty in the unit-cell volume, and consequently, the pressure axis in (b) is denoted by an error bar on $T_K^p(p)$. The solid line in (b) is a linear fit to $T_{\text{low}}^S(x)$.

Considering the Kondo and CEF energy scales of pure YbRh_2Si_2 , the two shoulders observed in the thermopower of $\text{Lu}_{1-x}\text{Yb}_x\text{Rh}_2\text{Si}_2$ ($x < 0.5$) are attributed to Kondo scattering on the ground-state doublet and on thermally populated multiplet states. Thus, the corresponding characteristic temperatures T_{low}^S and T_{high}^S allow an estimation of the evolution of T_K and Δ_{CEF} upon substitution. The position of the low- T minimum in the thermopower is usually close to the Kondo temperature of the CEF ground state,²⁰ in agreement with theoretical calculations for $s=1/2$ neglecting CEF effects.^{10,11} A recent calculation based on the single-impurity Anderson model including both a CEF splitting and charge fluctuations yielded a similar result.⁸ We therefore assume $T_{\text{low}}^S = T_K^S$. The high-temperature minimum is attributed to Kondo scattering from thermally populated CEF levels. Thus, it represents a characteristic temperature for the splitting of the relevant levels. Figure 3 shows the evolution of T_{low}^S and T_{high}^S upon substitution. They have been determined from a fit to the data between 4 and 200 K to a sum of two negative Gaussian curves on a logarithmic temperature scale.

Figure 3(a) displays T_{high}^S vs effective Yb content including the position of the single large minimum T_{min}^S in the thermopower of pure YbRh_2Si_2 . In view of the substantial uncertainty in the determination of T_{high}^S , the position of the high- T shoulder or minimum in $S(T)$ may be regarded as temperature independent. The mean value of 86 ± 10 K allows an estimate of the energetic position of the relevant excited CEF levels. As theoretical calculations predict $T_{\text{high}}^S = (0.3-0.6)\Delta_{\text{CEF}}/k_B$,^{8,12,13} the observed minimum corresponds to a splitting of 150–290 K with respect to the ground-state doublet. Thus, good agreement is obtained with results of inelastic neutron scattering, which revealed doublets at 0–200–290–500 K.⁴ We therefore conclude that the large thermopower minimum around 80 K is caused by Kondo scattering on the full Yb^{3+} multiplet.

Figure 3(b) shows the position of the low- T minimum $T_{\text{low}}^S = T_K^S$ of the samples with $x < 0.5$ vs x . For higher Yb concentrations, a determination of T_{low}^S was not possible with satisfactory precision. The data sets for low x clearly reveal an increasing T_K^S with rising Yb concentration. A linear extrapolation of $T_{\text{low}}^S(x)$ yields a Kondo temperature of 29 K for YbRh_2Si_2 . The fit is shown as a line in Fig. 3(b). This value is about a factor 1.5 larger than the one obtained from the entropy of the system, namely, $T_K^c = 17$ K.³ However, the model used in Ref. 3 for calculating T_K based on the entropy²¹ yields a temperature dependence of c_p , which deviates significantly from that of the NFL compound YbRh_2Si_2 . Its application to this system is therefore somewhat questionable. Furthermore, a determination of T_K from different experimental probes usually yields different values, however, always of the same order of magnitude.

The Lu-Yb substitution leads to a change in the unit-cell volume V_{uc} . In order to evaluate the relevance of this effect for the observed change in T_K , a comparison to results from experiments under pressure p are of interest. Using the bulk modulus²² of YbRh_2Si_2 of 189 GPa and assuming a linear relation of V_{uc} vs x , we can compare our results with investigations under pressure. The Kondo temperature $T_K^p(p)$ of YbRh_2Si_2 determined from resistive pressure studies²³ is shown as a dashed line in Fig. 3(b), where the pressure axis is scaled to the same unit-cell volume change. It is seen that the lowering of T_K under pressure is somewhat weaker than upon substitution. This reflects the relevance of additional effects beside the variation of V_{uc} . Chemical substitution induces a change in the band structure of the system, which may influence the effective coupling between the $4f$ and conduction electrons even at constant V_{uc} . However, the relatively small difference between the evolution of T_K under pressure and upon Lu substitution underlines a dominating influence of the unit-cell volume in $\text{Lu}_{1-x}\text{Yb}_x\text{Rh}_2\text{Si}_2$. This is ascribed to the unchanged chemical environment of the $4f$ moments as a result of the substitution on the rare-earth ion site. Furthermore, due to the small radius of the $4f$ shell, Lu and Yb behave chemically very similar. The $4f$ electrons together with the nucleus act as an “effective nucleus.” Therefore, Lu-Yb substitution is expected to have a minor influence on the band structure. Yet, the integer valence v of the Lu ions compared to the slightly reduced value for the Yb ions (Lu^{3+} vs Yb^{v+} with $2.95 \leq v \leq 3.00$)²⁴ might have a

small effect on the charge-carrier concentration.

The large values usually found for the thermopower of $4f$ systems have been related to the likewise enhanced electronic contributions to the specific heat. In the zero temperature limit, the ratio $S/\gamma T$ of several correlated compounds takes a quasiuniversal value.²⁵ For metals, the dimensionless quantity $q = N_{\text{Av}} e S / \gamma T$ with the Avogadro number N_{Av} and the electron charge e is close to ± 1 , whereas the sign depends on the type of charge carriers. This relation can be derived within Fermi-liquid theory assuming impurity scattering as the relevant scattering process.²⁶ In the present system, a thermopower $S \propto T$ is only found for $T < 5$ K and $x < 0.5$, due to both the low Kondo temperature of the order of 10 K and the NFL behavior of the pure system YbRh_2Si_2 . The calculated q values ranging from -0.63 to -0.85 are in line with that expected for holelike charge carriers of -1 .

The change in the behavior of $S(T)$ from a single minimum at $x=1$ to a double-peak structure for small x is correlated to the lowering of T_K upon decreasing Yb concentration. YbRh_2Si_2 with a Kondo temperature of approximately 20 K and a first excited CEF level around 200 K seems to be situated near the critical ratio T_{CEF}/T_K where the two minima of Kondo scattering on the ground state and thermally populated CEF levels in $S(T)$ merge into a single feature. A slight reduction of T_K on the other hand allows for a separation of both effects.

A similar behavior is found in the magnetic contribution to the resistivity $\rho_{\text{mag}}(T)$ of $\text{Lu}_{1-x}\text{Yb}_x\text{Rh}_2\text{Si}_2$. The similarities are best seen for the two samples with Yb concentrations at the crossover from a single large minimum in $S(T)$ to two clearly separated shoulders. Figure 4 shows a comparative plot of $S(T)$ as well as $\rho_{\text{mag}}(T)$, which were determined on the same specimens with $x=0.44$ and 0.62 . The curves for thermopower and magnetic resistivity strongly resemble each other. For the sample with $x=0.44$, two clearly separated shoulders are seen in both quantities, situated at the same temperatures, as indicated by the vertical lines. By contrast, the sample with $x=0.62$ exhibits only one large extremum in $S(T)$ and $\rho_{\text{mag}}(T)$ around 80 K. The double-peak structure is well tracked by both the thermopower and resistivity for $x < 0.5$, whereas larger concentrations $x > 0.5$ exhibit a single peak.

It appears remarkable that the effects of Kondo scattering on the ground-state doublet and on thermally populated CEF levels cannot be separated for $x > 0.5$ in $S(T)$ and $\rho(T)$, although the corresponding energy scales differ by approximately one order of magnitude. This observation can be understood in view of the relatively large temperature range, which is affected by the thermal population of an excited CEF level as apparent, e.g., from a Schottky contribution to the specific heat. A significant population of an excited CEF level and, consequently, an enhanced scattering from CEF excitations sets in at temperatures well below the splitting of Δ_{CEF}/k_B . Thus, in $\text{Lu}_{1-x}\text{Yb}_x\text{Rh}_2\text{Si}_2$, for $x > 0.5$, the crossover from scattering solely on the ground-state doublet to that on all CEF level may not be resolved. Instead, the observed single large extremum in $S(T)$ and $\rho(T)$ is caused by scattering on the full Yb^{3+} multiplet. On the other hand, in samples with $x < 0.5$, the reduced Kondo scale allows a separate ob-

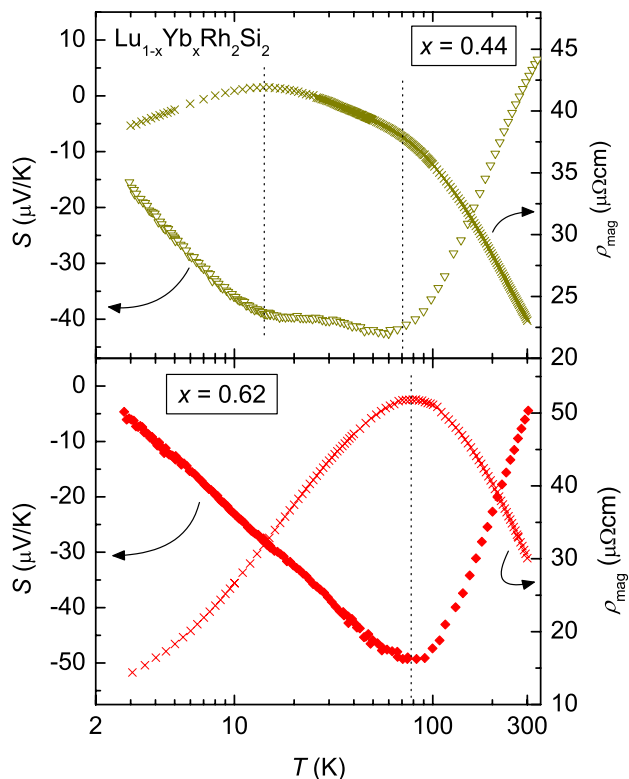


FIG. 4. (Color online) Comparison between thermopower and magnetic contributions to the resistivity for two Yb concentrations $x=0.44$ and $x=0.62$.

servation of scattering on the ground-state doublet at low T , while thermal population of the three excited levels gives rise to a second broad extremum at elevated temperatures.

The disappearance of the low- T minimum in the thermopower of $\text{Yb}(\text{Ni}_x\text{Cu}_{1-x})_2\text{Si}_2$ for $x=0$ is connected with a crossover to the valence-fluctuating regime.¹⁴ A qualitatively similar behavior has been frequently observed in Ce systems under pressure and upon substitution, e.g., in CeRu_2Ge_2 (Ref. 27) or $\text{Ce}(\text{Ni}_x\text{Pd}_{1-x})_2\text{Si}_2$.²⁸ In contrast to Yb compounds, Ce-based HF systems generally exhibit maxima in $S(T)$ due to the preponderance of electronlike charge carriers. Likewise, the crossover from two maxima to a single maximum is usually taken as an indication^{27,28} that T_K lies in the order of the CEF splitting and the system enters the valence-fluctuating regime. However, in x-ray absorption measurements of the L -III absorption edge of the Yb ion in $\text{Lu}_{1-x}\text{Yb}_x\text{Rh}_2\text{Si}_2$, no significant contribution from Yb^{2+} could be resolved at 5 K. Taking into account the resolution of the method, the valence v has been estimated to be $2.95 \leq v \leq 3.00$.²⁴ A strong intermediate-valent character is therefore excluded for this system. Thus, $\text{Lu}_{1-x}\text{Yb}_x\text{Rh}_2\text{Si}_2$ appears to be a rare example, for which the two extrema in $S(T)$ merge, while the system is still in the HF regime. The coalescence of both features corresponding to T_K and Δ_{CEF} can be observed in detail in this series since the Lu substitution induces an extremely small change of the unit-cell volume connected with a very weak lowering of T_K .

V. SUMMARY

The temperature dependence of the thermopower of $\text{Lu}_{1-x}\text{Yb}_x\text{Rh}_2\text{Si}_2$ qualitatively changes upon substitution from a single large minimum in $S(T)$ for the pure Yb compound to two well separated minima for $x < 0.5$. A similar evolution is found in the magnetic contribution to the resistivity. This change in the overall behavior of $S(T)$ and $\rho_{\text{mag}}(T)$ is ascribed to a lowering of T_K upon decreasing Yb content. For high Yb concentrations $x > 0.5$, the extrema of Kondo scattering on the ground state and thermally populated CEF levels merge into one single feature. A slight reduction of T_K due to the substitution of Yb by Lu on the other hand allows for a separation of both effects in the transport properties of the series for $x < 0.5$. The evolution of the Kondo temperature upon substitution can be understood mainly from the

change in the unit-cell volume. In addition, modifications in the band structure may be relevant. Due to the extremely small overall change in T_K , $\text{Lu}_{1-x}\text{Yb}_x\text{Rh}_2\text{Si}_2$ displays the crossover from two minima in $S(T)$ to one minimum upon increasing x without entering the valence-fluctuating regime. The Kondo temperature of YbRh_2Si_2 has been estimated to be around 29 K.

ACKNOWLEDGMENTS

We are grateful to V. Zlatić, S. Burdin, and C. Geibel for stimulating discussions. We thank N. Caroca-Canales for x-ray diffraction measurements on LuRh_2Si_2 . U.K. acknowledges financial support by COST action P16. Work at UC Irvine (S.M. and Z.F.) has been supported by NSF Grant No. DMR-0710492.

*koehler@cpfs.mpg.de

- ¹O. Trovarelli, C. Geibel, S. Mederle, C. Langhammer, F. M. Grosche, P. Gegenwart, M. Lang, G. Sparn, and F. Steglich, *Phys. Rev. Lett.* **85**, 626 (2000).
- ²P. Gegenwart, J. Custers, C. Geibel, K. Neumaier, T. Tayama, K. Tenya, O. Trovarelli, and F. Steglich, *Phys. Rev. Lett.* **89**, 056402 (2002).
- ³J. Ferstl, Ph.D. thesis, TU Dresden, 2007.
- ⁴O. Stockert, M. M. Koza, J. Ferstl, A. P. Murani, C. Geibel, and F. Steglich, *Physica B* **378-380**, 157 (2006).
- ⁵G. Dionicio, H. Wilhelm, G. Sparn, J. Ferstl, C. Geibel, and F. Steglich, *Physica B* **359-361**, 50 (2005).
- ⁶S. Hartmann, U. Köhler, N. Oeschler, S. Paschen, C. Krellner, C. Geibel, and F. Steglich, *Physica B* **378-380**, 70 (2006).
- ⁷K. Alami-Yadri, D. Jaccard, and D. Andreica, *J. Low Temp. Phys.* **114**, 135 (1999).
- ⁸V. Zlatić and R. Monnier, *Phys. Rev. B* **71**, 165109 (2005).
- ⁹Y. Lassailly, A. K. Bhattacharjee, and B. Coqblin, *Phys. Rev. B* **31**, 7424 (1985).
- ¹⁰N. E. Bickers, D. L. Cox, and J. W. Wilkins, *Phys. Rev. B* **36**, 2036 (1987).
- ¹¹G. D. Mahan, *Phys. Rev. B* **56**, 11833 (1997).
- ¹²A. K. Bhattacharjee and B. Coqblin, *Phys. Rev. B* **13**, 3441 (1976).
- ¹³S. Maekawa, S. Kashiba, M. Tachiki, and S. Takahashi, *J. Phys. Soc. Jpn.* **55**, 3194 (1986).
- ¹⁴D. Andreica, K. Alami-Yadri, D. Jaccard, A. Amato, and D. Schenck, *Physica B* **259-261**, 144 (1999).
- ¹⁵J. Ferstl, C. Geibel, F. Weickert, P. Gegenwart, T. Radu, T. Lühmann, and F. Steglich, *Physica B* **359-361**, 26 (2005).
- ¹⁶Z. Hossain, C. Geibel, F. Weickert, T. Radu, Y. Tokiwa, H. Jeevan, P. Gegenwart, and F. Steglich, *Phys. Rev. B* **72**, 094411 (2005).
- ¹⁷S. Mederle, R. Borth, C. Geibel, F. M. Grosche, G. Sparn, O. Trovarelli, and F. Steglich, *J. Phys.: Condens. Matter* **14**, 10731 (2002).
- ¹⁸S. Maquilon, Ph.D. thesis, UC Davis, 2007.
- ¹⁹Y. Ōnuki and T. Komatsubara, *J. Magn. Magn. Mater.* **63&64**, 281 (1987).
- ²⁰D. Huo, J. Sakurai, T. Kuwai, T. Mizushima, and Y. Isikawa, *J. Appl. Phys.* **89**, 7634 (2001).
- ²¹H.-U. Desgranges and K. D. Schotte, *Phys. Lett.* **91A**, 240 (1982).
- ²²J. Plessel, M. M. Abd-Elmeguid, J. P. Sanchez, G. Knebel, C. Geibel, O. Trovarelli, and F. Steglich, *Phys. Rev. B* **67**, 180403(R) (2003).
- ²³G. A. Dionicio, Ph.D. thesis, TU Dresden, 2006.
- ²⁴U. Burkhard (unpublished).
- ²⁵K. Behnia, D. Jaccard, and J. Flouquet, *J. Phys.: Condens. Matter* **16**, 5187 (2004).
- ²⁶K. Miyake and H. Kohno, *J. Phys. Soc. Jpn.* **74**, 254 (2005).
- ²⁷H. Wilhelm and D. Jaccard, *Phys. Rev. B* **69**, 214408 (2004).
- ²⁸D. Huo, J. Sakurai, O. Maruyama, T. Kuwai, and Y. Isikawa, *J. Magn. Magn. Mater.* **226-230**, 202 (2001).